

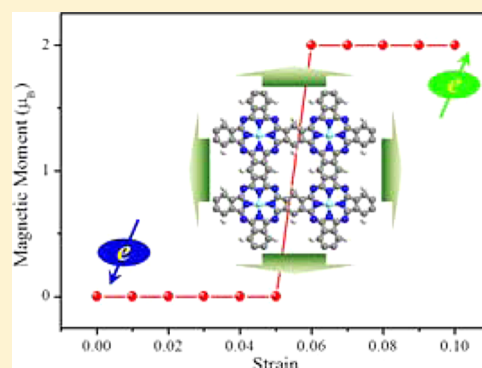
Strain-Induced Spin Crossover in Phthalocyanine-Based Organometallic Sheets

Jian Zhou,[†] Qian Wang,[‡] Qiang Sun,^{*,†,§} Yoshiyuki Kawazoe,^{||} and Puru Jena[§][†]Department of Materials Science and Engineering, College of Engineering, Peking University, Beijing 100871, China[‡]Center for Applied Physics and Technology, Peking University, Beijing 100871, China[§]Department of Physics, Virginia Commonwealth University, Richmond, Virginia 23284, United States^{||}Institute for Material Research, Tohoku University, Sendai, 980-8577, Japan

S Supporting Information

ABSTRACT: Motivated by the recent success in synthesizing two-dimensional Fe-phthalocyanine (poly-FePc) porous sheets, we studied strain-induced spin crossover in poly-TMPC (TM = Mn, Fe, Co, and Ni) systems by using first-principle calculations based on density functional theory. A small amount of biaxial tensile strain is found to not only significantly enhance the magnetic moment of the central TM atoms by $2 \mu_B$ when the strain reaches a critical value, but also the systems undergo low-spin (LS) to high-spin (HS) transition. These systems, however, show different response to strain, namely, poly-FePc sheet becomes ferromagnetic (FM) while poly-MnPc and poly-NiPc sheets become antiferromagnetic (AFM). Poly-CoPc, on the other hand, remains AFM. These predicted results can be observed in suspended poly-TMPC sheets by using scanning tunneling microscope (STM) tips to manipulate strain.

SECTION: Surfaces, Interfaces, Porous Materials, and Catalysis



A novel two-dimensional (2D) Fe embedded phthalocyanine (poly-FePc) organometallic porous sheet has been recently fabricated by Abel et al.¹ This provides the flexibility for synthesizing diverse TM-phthalocyanine-based (TMPC) organometallic sheets (poly-TMPC), since the central Fe atom can be easily substituted by other transition metal (TM) atoms.¹ The advantage of these systems is that the TM atoms are uniformly and separately distributed without clustering, and display well-fined geometry and magnetic properties. These systems are very different from the traditional dilute magnetic semiconductor (DMS) such as Ga(Mn,As) whose microstructure and magnetic behavior highly depend on the synthesis process.² Therefore, the poly-TMPC sheets are unique as compared with DMS, TM-doped graphene sheet, or BN sheet, showing great potential for applications in hydrogen storage,³ CO₂ capture,⁴ and spintronics.^{1,5} In our previous study,⁵ we systematically explored the magnetic properties of poly-TMPC sheets with 3d TM atoms (TM = Cr–Zn), and found that with the exception of TM = Ni and Zn which have a nonmagnetic (NM) ground state, the other TMPC sheets are magnetic. Each of the TM atoms, Cr, Mn, Fe, Co, Ni, Cu, and Zn, carries approximately 4, 3, 2, 1, 0, 1, and 0 μ_B magnetic moment, respectively. Moreover, MnPc sheet is ferromagnetic (FM), while for other sheets with TM = Cr, Fe, Co, and Cu, the coupling is antiferromagnetic (AFM). Since the interatomic separation between the TM atoms often determines their magnetic moment and coupling, we wondered if the magnetic

properties of these systems can be further tuned by external strain.

In this study we show that spin crossover (SCO) transition from a low-spin (LS) state to a high-spin (HS) state can be induced in the poly-TMPC sheets (where TM = Mn–Ni) by an external biaxial tensile strain. Conventional SCO has been observed in some single molecular magnets, which can be modulated mainly through temperature, irradiation, pressure, and external magnetic field.^{6–11} These molecules are generally composed of Fe or Co atoms coordinated with some ligands such as dithiocarbamate, where the TM atoms are in octahedral crystal field. Since the separated HS and LS states can be viewed as the two states of memory devices, the fast transition between the two states would provide high efficiency and high sensitivity for device applications. Using first principles calculations, we find that a small amount of biaxial tensile strain along the *x* and *y* directions can substantially enhance the magnetic moments of the central TM atoms from their ground (LS) state to a HS state. The magnetic moments of Mn, Fe, Co, and Ni increase by $2 \mu_B$. Following Hund's rule, the observed SCO is due to the occupation of $d_{x^2-y^2}$ orbital by a spin-up electron.

Received: August 30, 2012

Accepted: October 10, 2012

Published: October 10, 2012

Our first-principles calculations are based on spin polarized density functional theory (DFT) as implemented in the Vienna ab initio simulation package (VASP) code.¹² The exchange correlation functional is treated by generalized gradient approximation (GGA) in the form proposed by Perdew, Burke, and Ernzerhof (PBE).¹³ In order to treat strong correlation interactions between unfilled d orbitals of TM atoms, we apply the GGA+*U* scheme¹⁴ for the d electrons, while the delocalized s and p electrons are treated by the standard GGA method. The correlation energy *U* and the exchange energy *J* of the d electrons are set to be 4 and 1 eV, respectively, which has been well tested experimentally and theoretically for 3d TM system.^{2,5,15,16} We have also tested other *U* values (3 and 5 eV) for these systems, and similar SCO behavior was observed at different critical strains. The Vosko–Wilk–Nusair modification¹⁷ scheme is applied to interpolate the correlation energy in the spin polarized calculations. To treat the valence electrons, we use the projector augmented wave (PAW) method with a plane-wave basis set.^{18,19} The valence electron numbers of TM atoms are 7, 8, 9, and 10 for TM = Mn, Fe, Co, and Ni, respectively. In order to simulate 2D sheets, a periodic boundary condition is applied, and a vacuum space of 15 Å along the *z* direction is used to avoid interactions between nearest neighbor images. The structures are fully relaxed using the conjugated gradient method with no symmetry constraints. In order to calculate magnetic coupling between two TM atoms, a (2 × 2) supercell is considered. The reciprocal space is represented by the Monkhorst–Pack special k-point method²⁰ of 9 × 9 × 1 (or 5 × 5 × 1) meshes for one unit cell (or one supercell). The energy cutoff and convergence criteria for energy and force are set to be 400 eV, 1 × 10⁻⁴ eV, and 0.01 eV/Å, respectively. The accuracy of the above procedure has been carefully tested in our previous work.⁵

We previously found⁵ that the central TM atoms in poly-TMPc sheets are coordinated in a planar square crystal field, and the d orbitals split into “4 + 1” configurations, where *d_{xy}*, *d_{xz}*, *d_{yz}*, and *d_{z²}* orbitals have relatively comparable energies, and the *d_{x²-y²}* orbital has higher energy. It is known that the metal free Pc is in the form of H₂Pc to keep its aromaticity and flatness. Thus, each TM atom donates two 4s electrons and remains in the +2 valence state, as confirmed in previous studies.^{21–23} The total magnetic moments per unit cell of poly-MnPc, poly-FePc, poly-CoPc, and poly-NiPc sheets in their free states are then found to be 3, 2, 1, and 0 μ_B , respectively.⁵ Now we apply a biaxial tensile strain as shown by arrows in Figure 1. We find that the sheets keep their magnetic moments under small strain. However, each of their magnetic moments abruptly increases by 2 μ_B at some critical point. In order to study this phenomenon in more detail, we plot the total energy variations of poly-TMPc sheets in their LS state and HS state with respect to strain in Figure 2. Taking poly-MnPc sheet as an example, in its free state the ground state possesses 3 μ_B magnetic moment in one unit cell, while the HS state (5 μ_B) energy is slightly higher by 290 meV per unit cell. When we apply biaxial strain along the *x* and *y* directions, we observe a critical transition strain (denoted as σ_C) of about 1.9% beyond which the HS (5 μ_B) state has lower energy than the LS state, confirming an SCO transition from LS state to HS state. We find that further increasing the strain enhances the energy difference between the LS state and the HS state up to 10% strain. Similar behavior has also been found for poly-FePc, poly-CoPc, and poly-NiPc sheets, whose magnetic moments are increased to be 4, 3, and 2 μ_B , respectively. The corresponding

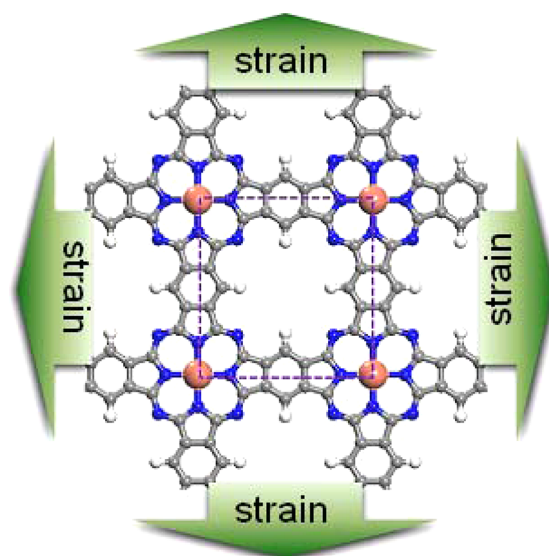


Figure 1. Geometric structure of poly-TMPc sheet under biaxial tensile strain. Dashed rectangle indicates one unit cell. White, gray, blue, and orange spheres denote H, C, N, and TM atoms, respectively.

σ_C parameters are 1.0%, 5.3%, and 6.8%, respectively. We have also calculated the required tensions to achieve these critical strains through $P = (dE/dS)$ and found that these values are all within 8 GPa·nm (Table 1). In particular, the NM poly-NiPc sheet becomes magnetic under the applied strain. Since the required strains are not too large, such transitions would be feasible in experiments, especially for the poly-MnPc and poly-FePc.

Next we examine the geometric, electronic, and magnetic properties of poly-TMPc sheets in their HS states under 10% tensile strain. We find that the tensions required to attain 10% strain are between 8.55 and 8.66 GPa·nm. The TM–N bond lengths are listed in Table 1. It can be seen that all the bond lengths are within 2.2 and 2.3 Å, which are longer than their corresponding values in free states by about 15%. We also observe Jahn–Teller distortion of four TM–N bonds in the poly-CoPc sheet. To illustrate their magnetic states, we plot the spin densities of the poly-TMPc sheets under 10% tensile strain in their HS states in Figure 3. The value of the isosurface is set to be 0.01 electron/Å³, the same as the spin density plot in our previous work.⁵ It can be clearly seen that the magnetism is still mainly associated with the d electrons of the central TM atoms, and their nearest neighbor N atoms are also spin polarized to some extent. In contrast to their free LS states, in the HS states the TM atoms and their coordinated N atoms have the same spin direction, and the other C and N atoms carry smaller magnetic moments.

Next we study the effect of biaxial tensile strain on magnetic couplings in these poly-TMPc sheets. To this end, we calculate exchange energy E_{ex} ($= E_{AFM} - E_{FM}$) in a (2 × 2) supercell as shown in Table 1. The positive and negative values of exchange energy indicate FM and AFM ground state of the sheet, respectively. We see that the poly-FePc sheet changes from AFM to FM (with exchange energy of 25 meV per supercell), while the reverse is the case with poly-MnPc. Poly-CoPc, on the other hand, remains AFM, and poly-NiPc is changed from NM to AFM. Therefore, strain is effective not only in changing the magnetic moments but also in altering the magnetic

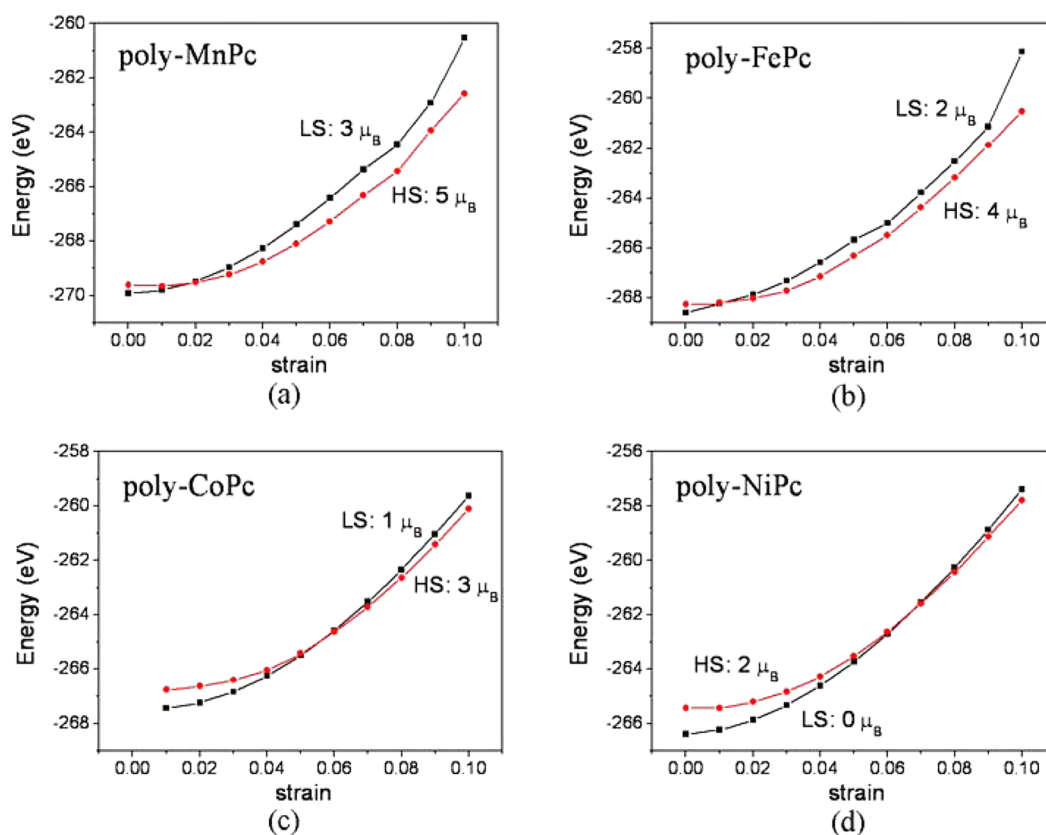


Figure 2. Total energy variations of two spin states with respect to the external strain of (a) poly-MnPc, (b) poly-FePc, (c) poly-CoPc, and (d) poly-NiPc sheets.

Table 1. Critical Strain (σ_C) Required to Transit from LS to HS and the Corresponding Tension (P_C)^a

	poly-MnPc	poly-FePc	poly-CoPc	poly-NiPc
σ_C	1.9%	1.0%	5.3%	6.8%
P_C (GPa•nm)	2.88	2.53	6.16	7.64
$d_{\text{TM-N}}$ (Å)	2.27	2.26	2.21/2.24	2.23
E_{ex} (meV)	-1	25	-11	-63
M (μ_B)	5	4	3	2

^aBond lengths between the central TM atoms and the neighboring N atoms ($d_{\text{TM-N}}$), exchange energies per supercell (E_{ex}), and total magnetic moments per unit cell (M) for 2D poly-TMPc sheets of the HS state at 10% tensile strain.

couplings. The mechanism responsible for this SCO transition will be discussed below.

The band structure and partial density of states (DOS) of an FM poly-FePc sheet are plotted in Figure 4, which shows that the poly-FePc is a semiconductor with a band gap of 0.55 eV. The valence band maximum (VBM) and conduction band minimum (CBM) are located at the M point ($=1/2, 1/2, 0$) of the reciprocal space, contributed by the delocalized p orbitals (dispersed bands). The d bands are flat (localized). We have also calculated the band structure of poly-MnPc, poly-CoPc, and poly-NiPc in their AFM states (see Supporting Information). It is found that the poly-MnPc is a semiconductor (with a band gap of 0.63 eV), while the poly-CoPc and poly-NiPc are metallic in both spin channels; the metallic bands are contributed by p electrons from Pc ligand frameworks. The d orbitals of all the systems exhibit semiconducting behavior.

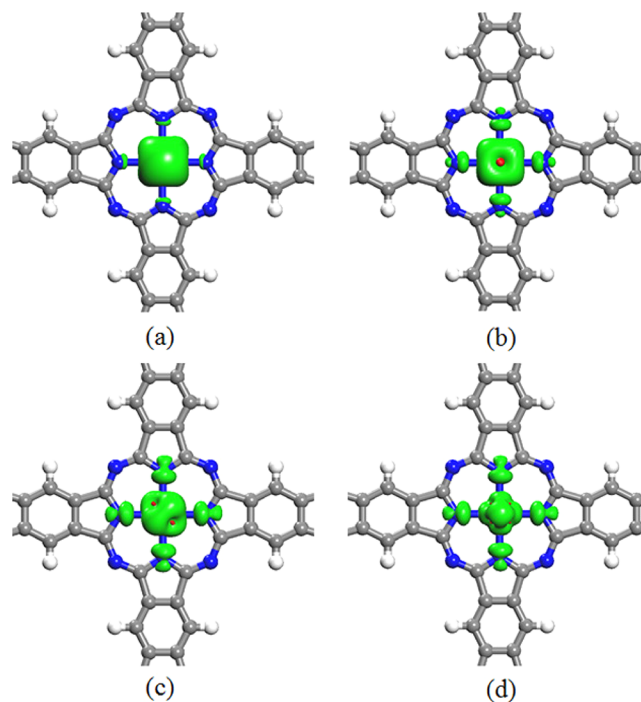


Figure 3. Spin densities of (a) poly-MnPc, (b) poly-FePc, (c) poly-CoPc, and (d) poly-NiPc sheets of the HS state in isosurface form with a value of 0.01 electron/Å³. Green and red colors represent spin-up and spin-down channels, respectively.

In order to analyze the SCO transition in detail, we plot the projected density of states (PDOS) of poly-TMPc sheets

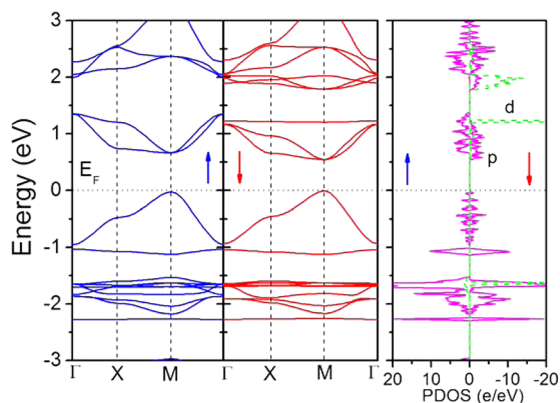


Figure 4. Band structure and partial DOS of an FM poly-FePc sheet.

corresponding to their ground magnetic states of 10% strain in Figure 5. For the poly-MnPc sheet, in contrast with the free LS state of poly-MnPc where the spin-up $d_{x^2-y^2}$ orbital is unoccupied and the spin-down d_{xy} is partially occupied, it is found that all five spin-up d orbitals are occupied, while all five spin-down d orbitals are unoccupied (Figure 5a). Because the tensile strain weakens the planar crystal field resulting in a decrease in the $d_{x^2-y^2}$ orbital energy level, the five valence electrons occupy the five spin-up d orbitals, while the five spin-down orbitals are all empty, according to Hund's rule. Thus, the total magnetic moment per unit cell is $5 \mu_B$. Similar behavior can be observed in the other three poly-TMPc sheets. For the poly-FePc sheet, the six valence d electrons occupy the five spin-up and the spin-down d_{z^2} orbitals, which results in a $4 \mu_B$ magnetic moment per unit cell (Figure 5b). When Co atoms are embedded, we find that the five spin-up d orbitals are

occupied, the spin-down d_{xy} and one d_{xy} orbital (d_{yz}) are occupied, leaving the other d_{xy} orbital (d_{xz}) empty (Figure 5c). This removes the double degeneracy of the d_{xy} orbitals, and a Jahn–Teller distortion occurs. As shown in Table 1, geometrically, the four Co–N bond lengths split into two groups. The two Co–N bonds in the x direction have shorter value, namely, 2.21 Å, while the two Co–N bonds in the y direction have longer value, namely, 2.24 Å. The total magnetic moment per unit cell decreases to $3 \mu_B$. Finally, for the poly-NiPc, all five spin-up orbitals and the spin-down d_{xy} and d_{yz} orbitals are occupied, leaving the spin-down d_{z^2} and $d_{x^2-y^2}$ orbitals empty. Additionally, the total magnetic moment is $2 \mu_B$ (Figure 5d). From the figure, we can also observe that, for the poly-MnPc, poly-CoPc, and poly-NiPc, the energy of the spin-up $d_{x^2-y^2}$ orbital is still relatively higher than the other occupied orbitals. However, for the poly-FePc, the spin-down d_{z^2} is slightly higher than the spin-up $d_{x^2-y^2}$ orbital. These partial d DOSs can be obtained by projecting DOS onto different d orbitals with different quantum numbers, while the positions of these orbitals are specified with peaks.

In order to check whether the 4s electrons transfer into the d orbitals of the TM ions, taking the poly-FePc system as an example, we integrated the projected d bands of Fe using $N = \int_{-\infty}^{E_F} n(E) dE$, where $n(E)$ and E_F are the d band DOS and the Fermi energy, respectively. We found that the total number of electrons in the d orbitals remains six. On the other hand, when similar calculations were performed on the 4s bands, we found that the total number of electrons in the s orbitals was less than two, indicating that the 4s electrons are transferred into the ligands, not into the empty d-orbitals.

It is interesting to ask whether other poly-TMPc sheets, for example, when TM = Cr, Cu, and Zn, can also have such SCO transition. These calculations were performed, and we found

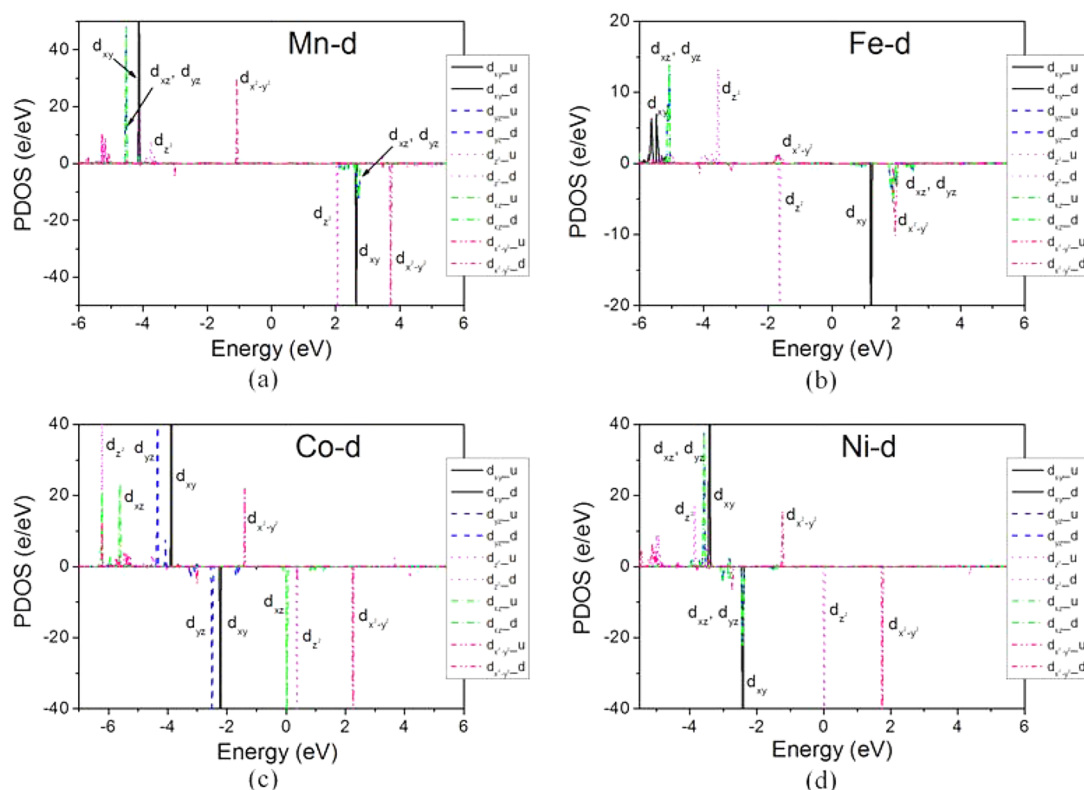


Figure 5. PDOS of d orbitals on the TM atom in a Pc sheet under a tensile strain: (a) Mn, (b) Fe, (c) Co, and (d) Ni.

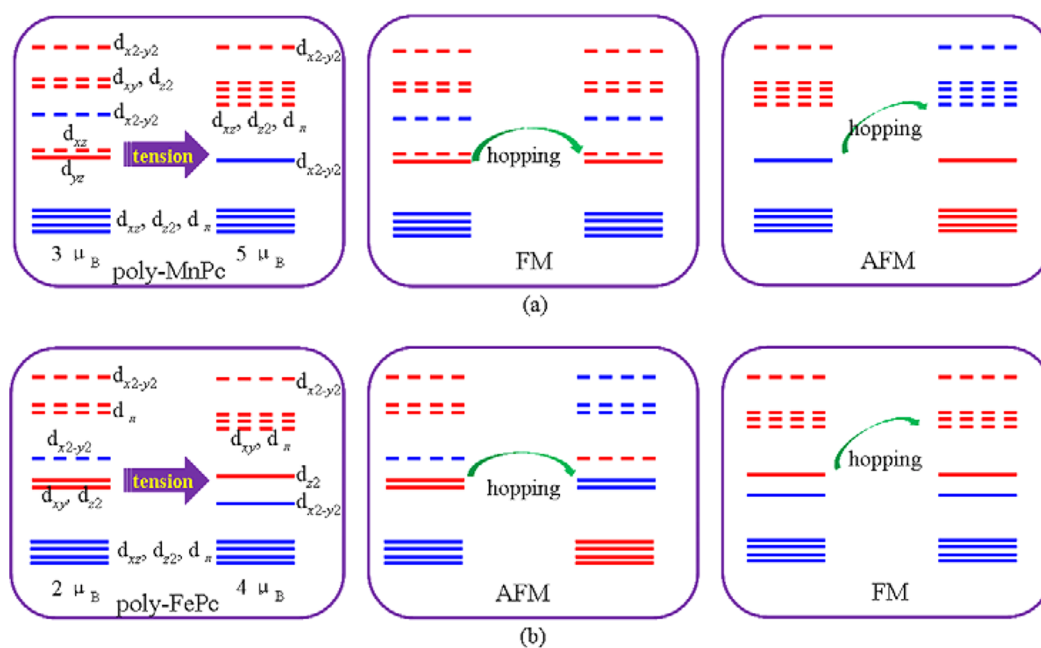


Figure 6. Illustration of energy levels of (a) poly-MnPc and (b) poly-FePc and their virtual hopping mechanisms. Left panel: energy level changes under tensile strain. Middle panel: virtual hopping mechanisms in the free LS states. Right panel: virtual hopping mechanisms in the HS states under tension. Blue and red lines represent spin-up and spin-down levels, respectively. Solid (dashed) line indicates occupied (unoccupied) state.

that the total magnetic moment did not change under even 10% tensile strain. This is because their orbital occupations still remain as in their free states, although the crystal field is weaker under strain. For the poly-CrPc, there are only four valence d electrons. Thus the $d_{x^2-y^2}$ will be always empty, and the magnetic moment remains at $4 \mu_B$. For poly-CuPc and poly-ZnPc in their free states, the spin-up $d_{x^2-y^2}$ orbital has been already occupied, so that the above-mentioned transition does not happen, leaving the total magnetic moment to be 1 and $0 \mu_B$, respectively.

We have discussed the changes in the magnetic moment under tension based on the orbital occupations. In the following, we briefly analyze their magnetic coupling behavior. For example, poly-MnPc and poly-FePc (Figure 6) undergo magnetic transitions from FM to AFM and from AFM to FM under biaxial tensile strain, respectively. For the poly-MnPc (Figure 6a), we see that in the LS state, the highest occupied and lowest unoccupied magnetic d orbitals are both in the spin-down channel, while under tensile strain the highest occupied magnetic d orbital is the spin-up $d_{x^2-y^2}$ orbital, and the lowest unoccupied orbital is the spin-down d_{z^2} orbital. Therefore, the poly-MnPc sheet in a LS state is FM due to virtual hopping between the frontier orbitals. This is consistent with our previous result.⁵ On the contrary, for the HS state under biaxial tensile strain, because the $d_{x^2-y^2}$ orbital is singly degenerate, the virtual hopping between two unit cells results in an AFM ground state. For the poly-FePc framework (Figure 6b), similar analysis can be done. In its LS state, the highest occupied state is the spin-down d_{z^2} orbital, while the lowest unoccupied state is the spin-up $d_{x^2-y^2}$ orbital. This leads to AFM coupling between each other.⁵ However, under biaxial tension, the highest occupied orbital (d_{z^2}) and lowest unoccupied orbital (d_{xy}) are both in the spin-down channel, and the FM state is more favorable than the AFM state. It is worth noting that such magnetic coupling analysis is also valid for the other poly-TMPc systems in their free LS and tensile HS states.

In summary, using DFT with GGA+*U*, we studied the effect of strain on magnetic properties of 2D porous poly-TMPc (TM = Mn, Fe, Co, and Ni) systems. We found that in these systems, the SCO transition from LS to HS state occurs when the tensile strain reaches 1.9%, 1.0%, 5.3%, and 6.8%, respectively. Simultaneously, the magnetic moments are increased by $2 \mu_B$ due to the occupation of the $d_{x^2-y^2}$ orbital. The N atoms bonded with TM become ferromagnetically polarized, and the magnetic coupling in poly-FePc changes from AFM to FM. On the other hand, poly-MnPc transitions to AFM from FM, and poly-NiPc transitions from NM to AFM. Poly-CoPc remains AFM, showing higher tolerance to the applied strain. The present study suggests that strain can be used as a variable to tune the magnetism of 2D phthalocyanine-based organometallic sheets.

■ ASSOCIATED CONTENT

📄 Supporting Information

Band structure of poly-MnPc, poly-CoPc, and poly-NiPc in their AFM state. This information is available free of charge via the Internet at <http://pubs.acs.org/>.

■ AUTHOR INFORMATION

✉ Corresponding Author

*E-mail: sunqiang@pku.edu.cn

Notes

The authors declare no competing financial interest.

■ ACKNOWLEDGMENTS

This work is partially supported by grants from the National Natural Science Foundation of China (NSFC-21173007, 11274023), from the National Grand Fundamental Research 973 Program of China (2012CB921404), from the United States Department of Energy, and from JST, CREST, “A mathematical challenge to a new phase of material sciences” (2008–2013). The authors thank the crew of the Center for

Computational Materials Science, the Institute for Materials Research, Tohoku University (Japan), for their continuous support of the HITACHSR11000 supercomputing facility.

REFERENCES

- (1) Abel, M.; Clair, S.; Ourdjini, O.; Mossoyan, M.; Porte, L. Single Layer of Polymeric Fe-Phthalocyanine: An Organometallic Sheet on Metal and Thin Insulating Film. *J. Am. Chem. Soc.* **2011**, *133*, 1203–1205.
- (2) Sato, K.; Bergqvist, L.; Kudrnovsky, J.; Dederichs, P. H.; Eriksson, O.; Turek, I.; Sanyal, B.; Bouzerar, G.; Katayama-Yoshida, H.; Dinh, V. A.; et al. First-Principles Theory of Dilute Magnetic Semiconductors. *Rev. Mod. Phys.* **2010**, *82*, 1633–1690.
- (3) Lü, K.; Zhou, J.; Zhou, L.; Wang, Q.; Sun, Q.; Jena, P. Sc-Phthalocyanine Sheet: Promising Material for Hydrogen Storage. *Appl. Phys. Lett.* **2011**, *99*, 163104–163106.
- (4) Lü, K.; Zhou, J.; Zhou, L.; Chen, X. S.; Chan, S. H.; Sun, Q. Pre-combustion CO₂ Capture by Transition Metal Ions Embedded in Phthalocyanine Sheets. *J. Chem. Phys.* **2012**, *136*, 234703–234709.
- (5) Zhou, J.; Sun, Q. Magnetism of Phthalocyanine-Based Organometallic Single Porous Sheet. *J. Am. Chem. Soc.* **2011**, *133*, 15113–15119.
- (6) Gutlich, P.; Goodwin, H. A. *Spin Crossover in Transition Metal Compounds*; Springer: New York, 2004.
- (7) Kahn, O.; Martinez, C. J. Spin-Transition Polymers: From Molecular Materials toward Memory Devices. *Science* **1998**, *279*, 44–48.
- (8) Halcrow, M. A. Structure: Function Relationships in Molecular Spin-Crossover Complexes. *Chem. Soc. Rev.* **2011**, *40*, 4119–4142.
- (9) Wolny, J. A.; Paulsen, H.; Trautwein, A. X.; Schünemann, V. Density Functional Theory Calculations and Vibrational Spectroscopy on Iron Spin-Crossover Compounds. *Coord. Chem. Rev.* **2009**, *253*, 2423–2431.
- (10) Bousseksou, A.; Molnar, G.; Salmon, L.; Nicolazzi, W. Molecular Spin Crossover Phenomenon: Recent Achievements and Prospects. *Chem. Soc. Rev.* **2011**, *40*, 3313–3335.
- (11) Hao, H.; Zheng, X.; Song, L.; Wang, R.; Zeng, Z. Electrostatic Spin Crossover in a Molecular Junction of a Single-Molecule Magnet Fe₂. *Phys. Rev. Lett.* **2012**, *108*, 017202–017206.
- (12) Kresse, G.; Furthmüller, J. Efficient Iterative Schemes for Ab Initio Total-Energy Calculations Using a Plane-Wave Basis Set. *Phys. Rev. B* **1996**, *54*, 11169–11186.
- (13) Perdew, J. P.; Burke, K.; Ernzerhof, M. Generalized Gradient Approximation Made Simple. *Phys. Rev. Lett.* **1996**, *77*, 3865–3868.
- (14) Dudarev, S. L.; Botton, G. A.; Savrasov, S. Y.; Humphreys, C. J.; Sutton, A. P. Electron-Energy-Loss Spectra and The Structural Stability of Nickel Oxide: An LSDA+*U* Study. *Phys. Rev. B* **1998**, *57*, 1505–1509.
- (15) Panchmatia, P. M.; Sanyal, B.; Oppeneer, P. M. GGA + *U* Modeling of Structural, Electronic, and Magnetic Properties of Iron Porphyrin-Type Molecules. *Chem. Phys.* **2008**, *343*, 47–60.
- (16) Okabayashi, J.; Okabayashi, J.; Rader, O.; Mizokawa, T.; Fujimori, A.; Hayashi, T.; Tanaka, M. Core-Level Photoemission Study of Ga_{1-x}Mn_xAs. *Phys. Rev. B* **1998**, *58*, R4211–R4214.
- (17) Vosko, S. H.; Wilk, L.; Nusair, M. Accurate Spin-Dependent Electron Liquid Correlation Energies for Local Spin Density Calculations: a Critical Analysis. *Can. J. Phys.* **1980**, *58*, 1200–1211.
- (18) Blochl, P. E. Projector Augmented-Wave Method. *Phys. Rev. B* **1994**, *50*, 17953–17979.
- (19) Kresse, G.; Joubert, D. From Ultrasoft Pseudopotentials to the Projector Augmented-Wave Method. *Phys. Rev. B* **1999**, *59*, 1758–1775.
- (20) Monkhorst, H. J.; Pack, J. D. Special Points for Brillouin-Zone Integrations. *Phys. Rev. B* **1976**, *13*, 5188–5192.
- (21) Bhattacharjee, S.; Brena, B.; Banerjee, R.; Wende, H.; Eriksson, O.; Sanyal, B. Electronic Structure of Co-Phthalocyanine Calculated by GGA+*U* and Hybrid Functional Methods. *Chem. Phys.* **2010**, *377*, 96–99.
- (22) Liao, M.-S.; Scheiner, S. Electronic Structure and Bonding in Metal Phthalocyanines, Metal = Fe, Co, Ni, Cu, Zn, Mg. *J. Chem. Phys.* **2001**, *114*, 9780–9791.
- (23) Isvoranu, C.; Wang, B.; Ataman, E.; Schulte, K.; Knudsen, J.; Andersen, J. N.; Bocquet, M.-L.; Schnadt, J. Pyridine Adsorption on Single-Layer Iron Phthalocyanine on Au(111). *J. Phys. Chem. C* **2011**, *115*, 20201–20208.